



Novel 2-Arylbenzimidazole derivatives as multi-targeting agents to treat Alzheimer's disease

Oya Unsal-Tan¹ · Keriman Ozadali-Sari¹ · Beyza Ayazgok² · Tuba Tüylü Küçükkuşç² · Ayla Balkan¹

Received: 21 November 2016 / Accepted: 10 March 2017
© Springer Science+Business Media New York 2017

Abstract This study describes the synthesis, pharmacological evaluation, including acetylcholinesterase (AChE)/butyrylcholinesterase (BChE) inhibition, amyloid beta (A β) antiaggregation, and neuroprotective effects, as well as molecular modeling of novel 2-(4-substituted phenyl)-1*H*-benzimidazole derivatives. These derivatives were synthesized by cyclization of *o*-phenylenediamines with sodium hydroxy(4-substituted phenyl)methanesulfonate salts. In vitro studies indicated that the most of the target compounds showed remarkable inhibitory activity against BChE (IC₅₀: 13.60–95.44 μ M). Among them, **3d** and **3g-i** also exhibited high selectivity (SI \geq 35.7) for BChE with IC₅₀ values 39.56, 13.60, 14.45, and 15.15 μ M, respectively. According to the molecular modeling studies, it may be assumed that the compounds are able to reach the catalytic site of BChE but not that of AChE. The compounds showing BChE inhibitory effects were subsequently examined for their A β -antiaggregating and neuroprotective activities. Among the compounds, **3d** inhibited the A β _{1–40} aggregation and demonstrated significant neuroprotection against H₂O₂-induced and A β _{1–40}-induced cell death. Collectively, compound **3d** showed the best multifunctional activity (BChE; IC₅₀ = 39.56 μ M, SI > 126; A β self-mediated aggregation;

67.78% at 100 μ M; H₂O₂-induced cytotoxicity with cell viability of 98% and A β _{1–40}-induced cytotoxicity with cell viability of 127%). All these results suggested that 2-(4-(4-methylpiperidin-1-yl)phenyl)-1*H*-benzo[*d*]imidazole (compound **3d**) could be a promising multi-target lead candidate against Alzheimer's disease.

Keywords 2-Arylbenzimidazole · Alzheimer's disease · Butyrylcholinesterase · A β aggregation · Neuroprotection

Introduction

Alzheimer's disease (AD) is a progressive and irreversible neurodegenerative brain disorder and the most common type of dementia. It is known that some factors seem to play a significant role in the pathology of AD, such as low levels of acetylcholine (ACh), β -amyloid (A β) aggregation, tau protein phosphorylation, increased oxidative stress and neuroinflammation of the central nervous system. Two main mechanisms have been proposed for the pathogenesis of the disease, a cholinergic hypothesis and amyloid cascade hypothesis (Oddo et al. 2003; Taylor et al. 2002; Cummings 2004; Anand and Singh 2013; Manev et al. 2011).

The cholinergic hypothesis is based on reduced ACh levels in the brain of AD patients, which leads to a decline in cognitive skills and memory. Cholinesterase (ChE) inhibitors such as galantamine, rivastigmine, and donepezil are commonly used to increase the ACh levels and improve cholinergic functions. However, the efficacy of all these inhibitors is clinically limited (Anand and Singh 2013; Yiannopoulou and Papageorgiou 2013). In the healthy brain, acetylcholinesterase (AChE) is the main enzyme

Electronic supplementary material The online version of this article (doi:10.1007/s00044-017-1874-1) contains supplementary material, which is available to authorized users.

✉ Oya Unsal-Tan
oyaunsal@hacettepe.edu.tr

¹ Faculty of Pharmacy, Department of Pharmaceutical Chemistry, Hacettepe University, Ankara, Turkey

² Faculty of Pharmacy, Department of Biochemistry, Hacettepe University, Ankara, Turkey

responsible for ACh hydrolysis, which terminates neurotransmission. Butyrylcholinesterase (BChE) is a scavenging enzyme, which substitutes for AChE when necessary. In the AD brain, the BChE activity rises, while that of AChE remains unchanged or declines (Perry et al. 1978; Giacobini 2003).

A randomized controlled trial of 998 patients has shown that the dual ChE inhibitor rivastigmine is more beneficial than the selective AChE inhibitor donepezil (Bullock et al. 2005). BChE knockout studies showed unchanged cognitive properties (Holmes et al. 2005) and a decrease in fibrillar A β (Reid and Darvesh 2015; Darvesh and Reid 2016). Thus, inhibition of BChE may be important for treatment of AD by raising ACh levels and decreasing fibrillar A β in the brain.

The amyloid hypothesis states that the assembly of A β into oligomers and fibrils is one of the hallmarks in the progression of AD, leading to neuronal cell death and secondary events such as neuroinflammation which contributes to the neurodegeneration (Sun et al. 2015; Huang et al. 2015). Despite the effort during last two decades, researchers have not been successful either in the clinical trials for anti A β drugs or in the explanation of amyloid mechanism in AD (Karran et al. 2011). But there is no doubt that AD pathogenesis is strongly related to the abnormal accumulation and aggregation A β . Thus, targeting A β is still thought to be a pivotal strategy for AD treatment (Gouras et al. 2015; Selkoe and Hardy 2016; Mullard 2017).

Benzimidazoles have many useful therapeutic activities, such as antiviral, antihistaminic, anticancer, antiulcer, anti-hypertensive, antidiabetic, antifungal, antimicrobial, and antiinflammatory (Yadav and Ganguly 2015; Bansal and Silakari 2012; Secci et al. 2012). Despite being a privileged scaffold in medicinal chemistry, benzimidazoles have not been considered for their ChE inhibitory activities, with only a few studies published in recent years (Alpan et al. 2013; Zhu et al. 2013; Yoon et al. 2013).

Although there is no evidence that the benzimidazoles possess any inhibitory effect on A β aggregates, some reports emphasized that benzimidazole derivatives containing amine side chains (Fig. 1) can be used as amyloid imaging probes due to their high binding affinity to A β aggregates and high uptake into the brain (Cui et al. 2011; Harada et al. 2014).

A multitarget-directed ligand (MTDL) strategy has been developed for the treatment of disorders with complex pathological mechanisms, such as AD. Since the exact neuropathogenesis of AD is not fully known, selecting biological targets for AD is difficult. However, among others, ChE and A β are considered the most significant targets for the development of novel MTDLs today.

The aim of the present study was to obtain novel MTDLs by combining BChE and A β aggregation inhibitory activities

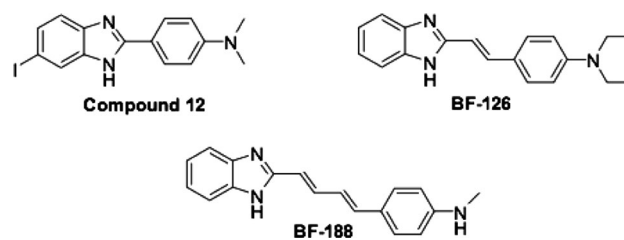


Fig. 1 Benzimidazole derivatives with high-binding affinity to A β aggregates

in one neuroprotective structure. For this purpose, we designed, synthesized, and biologically evaluated some 2-phenylbenzimidazole derivatives carrying aliphatic/aromatic amine side chains as MTDLs for AD treatment. The biological evaluation of the benzimidazoles included AChE/BChE inhibition, self-induced A β aggregation, and neuroprotection.

Materials and methods

Chemistry

Melting points were determined with a Thomas—Hoover capillary melting point apparatus (Thomas Scientific, Philadelphia, PA, USA) and were not corrected. Attenuated total reflection (ATR)—Fourier transform IR (FTIR) spectra were obtained using a MIRacle ATR accessory (Pike Technologies, Fitchburg, WI, USA) in conjunction with a Spectrum BX FTIR spectrometer (Perkin Elmer, USA) and were reported in cm^{-1} . $^1\text{H-NMR}$ and $^{13}\text{C-NMR}$ spectra (Dimethyl sulfoxide (DMSO)- d_6) were recorded on a Varian Mercury 400 FT NMR spectrophotometer using tetramethylsilane as an internal reference (chemical shift represented in δ p.p.m.). ESI—MS spectra were measured on a micromass ZQ-4000 single—quadrupole mass spectrometer. Elemental analyses (C, H, and N) were performed on Leco CHNS 932 analyzer (Leco, St. Joseph, MI, USA).

General procedure for the preparation of 4-substituted-benzaldehydes (1a–e)

4-Fluorobenzaldehyde and appropriate amine derivatives were reacted in the presence of potassium carbonate in DMSO as mentioned in the literature (Meciarova et al. 2003).

General procedure for the preparation of sodium hydroxy (4-substituted phenyl)methanesulfonate salts (2a–e)

Substituted benzaldehydes (0.04 mol) and sodium bisulfite (0.04 mol), dissolved in 20 mL of an ethanol and water

mixture, were stirred for 1 h at room temperature. The formed sodium hydroxy(4-substituted phenyl)methanesulfonate salts were obtained by filtration.

General procedure for the preparation of 2-(4-substitutedphenyl)-1H-benzimidazole derivatives (3a–j)

The crude sodium hydroxy(4-substituted phenyl)methanesulfonate salts (0.01 mol) and *o*-phenylenediamine (0.01 mol) were refluxed in 30 mL of dimethyl formamide for 2–4 h. After monitoring by thin-layer chromatography, the mixture was cooled to room temperature and poured into ice water. The obtained 1H-benzimidazoles were filtered and recrystallized from methanol/water.

2-(4-(1H-1,2,4-Triazol-1-yl)phenyl)-1H-benzo[d]imidazole (**3a**) M.p. 105 °C (m.p. 102–104 °C) (Jadhav et al. 2009).

2-(4-(1H-Imidazol-1-yl)phenyl)-1H-benzo[d]imidazole (**3b**) M.p. 215 °C. (Yu et al. 2013)

2-(4-(1H-Benzo[d]imidazol-1-yl)phenyl)-1H-benzo[d]imidazole (**3c**) M.p. 196 °C (m.p. 199–200 °C) (Alp et al. 2014).

2-(4-(4-Methylpiperidin-1-yl)phenyl)-1H-benzo[d]imidazole (**3d**) Yellow solid; yield 76%; m.p. 183 °C; IR (cm^{-1}); 2924, 1604, 1506, 1461; $^1\text{H-NMR}$ (DMSO, 400 MHz); 0.93 (3H; d; CH_3 , J : 6.8), 1.13–1.23 (2H; qd; NCH_2CH_2 , J : 12.6/3.6), 1.56–1.61 (1H; m; NCH_2CH_2), 1.69 (2H; d_{br}; NCH_2CH_2 , J : 12.8), 2.82 (2H; td; NCH_2 , J : 12.4/2.4), 3.92 (2H; d_{br}; NCH_2 , J : 12.8), 7.11 (2H; d; 3'-HAr and 5'-HAr, J : 9.2), 7.29–7.26 (2H; m; 4-HAr and 7-HAr), 7.61–7.59 (2H; m; 5-HAr and 6-HAr), 8.00 (2H; d; 2'-HAr and 6'-HAr, J : 8.8); $^{13}\text{C-NMR}$ (DMSO, 100 MHz); 21.7 (CH_3), 30.3 (CH), 33.1 (CH_2), 47.4 (CH_2), 113.9, 114.3, 114.9, 123.0, 128.3, 136.2, 150.9, 152.5. ESI-MS (m/z); 314.23 $[\text{M} + \text{Na}]^+$, 292.26 $[\text{M} + \text{H}]^+$; Anal. Calcd. for $\text{C}_{19}\text{H}_{21}\text{N}_3$: C, 78.32; H, 7.26; N, 14.42. Found: C, 77.99; H, 7.32; N, 14.11.

2-(4-(4-Benzylpiperidin-1-yl)phenyl)-1H-benzo[d]imidazole (**3e**) Yellow solid; yield 65%; m.p. 187 °C; IR (cm^{-1}); 2923, 1607, 1497, 1439; $^1\text{H-NMR}$ (DMSO, 400 MHz); 1.22–1.32 (2H; qd; NCH_2CH_2 , J : 12/3.6), 1.65 (2H; brd; NCH_2CH_2 , J : 14), 1.70–1.75 (1H; m; NCH_2CH_2), 2.54 (2H; d; CH_2Ph , J : 7.2), 2.72 (2H; td; NCH_2 , J : 11.4/1.2), 3.84 (2H; brd; NCH_2 , J : 12.8), 7.04 (2H; d; 3'-HAr and 5'-HAr, J : 9.2), 7.12–7.15 (2H; m; 4-HAr and 7-HAr), 7.17–7.20 (2H; m; Ar), 7.28–7.31 (3H; m; Ar), 7.50–7.53 (2H; m; 5-HAr and 6-HAr), 7.98 (2H; d; 2'-HAr and 6'-HAr, J : 9.2); $^{13}\text{C-NMR}$ (DMSO, 100 MHz); 31.1 (CH_2), 37.3 (CH), 42.2 (CH_2), 47.7 (CH_2), 114.7,

119.1, 121.4, 125.8, 127.5, 129.0, 140.1, 151.8, 151.9. ESI-MS (m/z); 390.17 $[\text{M} + \text{Na}]^+$, 368.18 $[\text{M} + \text{H}]^+$; Anal. Calcd. for $\text{C}_{25}\text{H}_{25}\text{N}_3$: C, 81.71; H, 6.86; N, 11.43. Found: C, 81.69; H, 7.12; N, 11.30.

5-Methoxy-2-(4-(1H-1,2,4-triazol-1-yl)phenyl)-1H-benzo[d]imidazole (**3f**) Yellow solid; yield 86%; m.p. 148 °C; IR (cm^{-1}); 3111, 1633, 1513, 1453; $^1\text{H-NMR}$ (DMSO, 400 MHz); 3.82 (3H; s; OCH_3), 6.87–6.89 (1H; dd; 6-HAr, J : 8.8/2), 7.10 (1H; d; 4-HAr, J : 2), 7.53 (1H; d; 7-HAr, J : 8.8), 8.07 (2H; d; 3'-HAr and 5'-HAr, J : 8.8), 8.29–8.31 (3H; m; triazole, 2'-HAr and 6'-HAr), 9.40 (1H; s; triazole); $^{13}\text{C-NMR}$ (DMSO, 100 MHz); 55.5 (CH_3), 112.3, 119.7, 127.6, 128.8, 137.4, 142.5, 149.5, 152.6, 156.2. ESI-MS (m/z); 314.39 $[\text{M} + \text{Na}]^+$, 292.40 $[\text{M} + \text{H}]^+$; Anal. Calcd. for $\text{C}_{16}\text{H}_{13}\text{N}_5\text{O}$: C, 65.97; H, 4.50; N, 24.04. Found: C, 65.71; H, 4.56; N, 23.88.

5-Methoxy-2-(4-(1H-imidazol-1-yl)phenyl)-1H-benzo[d]imidazole (**3g**) Yellow solid; yield 82%; m.p. 173 °C; IR (cm^{-1}); 3357, 3108, 1636, 1611, 1515, 1479; $^1\text{H-NMR}$ (DMSO, 400 MHz); 3.84 (3H; s; OCH_3), 6.96–6.99 (1H; dd; 6-HAr, J : 8.8/2.4), 7.16 (1H; d; 4-HAr, J : 2.4), 7.61 (1H; d; 7-HAr, J : 8.8), 7.74 (1H; s; imidazole), 8.04 (2H; d; 3'-HAr and 5'-HAr, J : 8.4), 8.27 (1H; s; imidazole), 8.45 (2H; d; 2'-HAr and 6'-HAr, J : 8.4), 9.45 (1H; s; imidazole); $^{13}\text{C-NMR}$ (DMSO, 100 MHz); 55.6 (CH_3), 96.8, 113.6, 115.7, 119.6, 121.7, 123.9, 127.5, 128.3, 131.4, 134.9, 136.9, 148.3, 156.8. ESI-MS (m/z); 313.39 $[\text{M} + \text{Na}]^+$, 291.40 $[\text{M} + \text{H}]^+$; Anal. Calcd. for $\text{C}_{17}\text{H}_{14}\text{N}_4\text{O}$: C, 70.33; H, 4.86; N, 19.30. Found: C, 70.09; H, 5.11; N, 19.43.

5-Methoxy-2-(4-(1H-benzo[d]imidazol-1-yl)phenyl)-1H-benzo[d]imidazole (**3h**) Yellow solid; yield 80%; m.p. 185 °C; IR (cm^{-1}); 3064, 1639, 1606, 1494, 1454; $^1\text{H-NMR}$ (DMSO, 400 MHz); 3.86 (3H; s; OCH_3), 6.98–7.01 (1H; dd; 6-HAr, J : 8.8/2.4), 7.19 (1H; d; 4-HAr, J : 2.4), 7.35–7.43 (2H; m; 5-Hbenzimidazole and 6-Hbenzimidazole), 7.63 (1H; d; 7-HAr, J : 8.8), 7.78 (1H; dd; 7-Hbenzimidazole, J : 6.8/1.6), 7.83 (1H; dd; 4-Hbenzimidazole, J : 6.8/1.6), 7.98 (2H; d; 3'-HAr and 5'-HAr, J : 8.4), 8.38 (2H; d; 2'-HAr and 6'-HAr, J : 9.2), 8.78 (1H; s; 2-Hbenzimidazole); $^{13}\text{C-NMR}$ (DMSO, 100 MHz); 55.6 (CH_3), 94.3, 97.1, 110.9, 113.0, 115.8, 119.8, 122.8, 123.8, 123.9, 127.4, 128.1, 132.6, 137.3, 137.6, 143.0, 143.3, 149.1, 156.6. ESI-MS (m/z); 363.39 $[\text{M} + \text{Na}]^+$, 341.41 $[\text{M} + \text{H}]^+$; Anal. Calcd. for $\text{C}_{21}\text{H}_{16}\text{N}_4\text{O}$: C, 74.10; H, 4.74; N, 16.46. Found: C, 73.95; H, 5.02; N, 16.33.

5-Methoxy-2-(4-(4-methylpiperidin-1-yl)phenyl)-1H-benzo[d]imidazole (**3i**) Yellow solid; yield 77%; m.p. 156 °C; IR (cm^{-1}); 2923, 1606, 1504, 1454; $^1\text{H-NMR}$ (DMSO, 400 MHz); 0.93 (3H; d; CH_3 , J : 6.8), 1.18–1.25

(2H; qd; $\text{NCH}_2\text{CH}_{2\text{ax}}$, J : 12.4/3.6), 1.56–1.58 (1H; m; $\text{NCH}_2\text{CH}_2\text{CH}$), 1.69 (2H; brd; $\text{NCH}_2\text{CH}_{2\text{eq}}$, J : 12.4), 2.76 (2H; td; $\text{NCH}_{2\text{ax}}$, J : 12.4/2.4), 3.79 (3H; s; OCH_3), 3.84 (2H; brd; $\text{NCH}_{2\text{eq}}$, J : 12.8), 6.78–6.81 (1H; dd; 6-HAr, J : 8.4/2.4), 7.02–7.06 (3H; m; 3'-HAr, 5'-HAr and 4-HAr), 7.41 (1H; d; 7-HAr, J : 8.8), 7.94 (2H; d; 2'-HAr and 6'-HAr, J : 8.8); ^{13}C -NMR (DMSO, 100 MHz); 21.7 (CH_3), 30.3 (CH), 33.2 (CH_2), 47.8 (CH_2), 55.4 (CH_3), 110.9, 114.7, 118.5, 127.4, 151.4, 151.8, 155.6. ESI-MS (m/z); 344.47 $[\text{M} + \text{Na}]^+$, 322.50 $[\text{M} + \text{H}]^+$; Anal. Calcd. for $\text{C}_{20}\text{H}_{23}\text{N}_3\text{O}$: C, 74.74; H, 7.21; N, 13.07. Found: C, 75.02; H, 7.18; N, 13.41.

5-Methoxy-2-(4-(4-benzylpiperidin-1-yl)phenyl)-1H-benzimidazole (**3j**) Yellow solid; yield 79%; m.p. 143 °C; IR (cm^{-1}); 2928, 1635, 1605, 1506, 1475; ^1H -NMR (DMSO, 400 MHz); 1.21–1.30 (2H; qd; $\text{NCH}_2\text{CH}_{2\text{ax}}$, J : 12/3.2), 1.66 (2H; brd; $\text{NCH}_2\text{CH}_{2\text{eq}}$, J : 12.8), 1.75–1.80 (1H; m; $\text{NCH}_2\text{CH}_2\text{CH}$), 2.54 (2H; d; CH_2Ph , J : 7.2), 2.80 (2H; t; $\text{NCH}_{2\text{ax}}$, J : 12), 3.83 (3H; s; OCH_3), 3.92 (2H; brd; $\text{NCH}_{2\text{eq}}$, J : 12.8), 6.92–6.95 (1H; dd; 6-HAr, J : 8.8/2.4), 7.07–7.09 (3H; m; Ar and 4-HAr), 7.18–7.20 (3H; m; Ar and 3'-HAr and 5'-HAr), 7.27–7.31 (2H; m; Ar), 7.51 (1H; d; 7-HAr, J : 8.8), 8.01 (2H; d; 2'-HAr and 6'-HAr, J : 9.2); ^{13}C -NMR (DMSO, 100 MHz); 31.5 (CH_2), 37.8 (CH), 42.6 (CH_2), 47.8 (CH_2), 56.1 (CH_3), 97.2, 113.1, 114.8, 115.1, 126.3, 128.6, 128.7, 129.5, 136.5, 140.6, 150.6, 153.0, 157.0. ESI-MS (m/z); 420.50 $[\text{M} + \text{Na}]^+$, 398.51 $[\text{M} + \text{H}]^+$; Anal. Calcd. for $\text{C}_{26}\text{H}_{27}\text{N}_3\text{O}$: C, 78.56; H, 6.85; N, 10.57. Found: C, 78.32; H, 7.10; N, 10.50.

Biological assays

Cholinesterase inhibitory activity

Acetylcholinesterase human recombinant (C1682), butyrylcholinesterase from equine serum (C1057), acetylthiocholine iodide (A5751), and S-butyrylthiocholine iodide (B3253) were obtained from Sigma—Aldrich, and 5,5'-dithiobis(2-nitrobenzoic acid) (DTNB) was from Calbiochem (Los Angeles, CA, USA). IC_{50} values of the novel benzimidazole derivatives were determined by the Ellman's assay (Ellman et al. 1961). Reactions were initiated by the addition of an enzyme into a medium containing the substrate (0.05–0.4 mM) and 0.125 mM DTNB in 100 mM 3-(*N*-morpholino)propanesulfonic acid buffer, pH 8.0, at 25 °C and monitored spectrophotometrically at 412 nm in a UV-visible 1700 Shimadzu PC spectrophotometer. Dose-response curves were plotted using the GraphPad Prism 5 software. An enzyme kinetic assay was performed for compound **3g** at different butyrylthiocholine (BTC) concentrations (0.1–0.5 mM). Donepezil—HCl (Sigma) was tested as a reference compound.

Amyloid peptide preparation

$\text{A}\beta_{1-40}$ protein fragment (A1075, Sigma—Aldrich) was dissolved in phosphate-buffered saline (PBS), pH 7.4, at a concentration of 50 μM and incubated at 37 °C for seven days to induce peptide aggregation.

Inhibition of $\text{A}\beta_{1-40}$ aggregation

$\text{A}\beta_{1-40}$ -destabilizing effects were determined for the compounds with IC_{50} values lower than 100 μM for both ChEs. $\text{A}\beta_{1-40}$ (10 μL) was added to the assay medium containing 0.01 M NaCl in 0.05 M potassium phosphate buffer, pH 7.4, and incubated at 37 °C for 48 h in the absence and presence of the inhibitors (100 μM). The incubated $\text{A}\beta_{1-40}$ (100 μL) was mixed with 50 μL of thioflavin T (ThT; 200 μM) in 50 mM glycine—NaOH buffer (pH 8.5). Inhibition of $\text{A}\beta$ aggregation was evaluated by the decrease of ThT fluorescence intensity at the excitation wavelength of 448 nm and emission wavelength of 490 nm using an RF 5301 PC spectrofluorophotometer. Rifampicin and donepezil (100 μM) were tested as reference compounds.

Cell culture

Fetal bovine serum (FBS; S181G-500) and 200 mM L-glutamine (17-605E) for cell culture were obtained from Biowest and Lonza, respectively. HyClone 0.25% 1 \times trypsin (SV30031.01) and HyClone PBS (SH30256.01) were purchased from Thermo Scientific. DMSO (67-68-5) was obtained from Merck. SH-SY5Y human neuroblastoma cells were cultured in Dulbecco's modified Eagle's medium (DMEM) supplemented with 10% FBS, 1% L-glutamine, and 1% antibiotic mix. Cells were maintained at 37 °C in a humidified atmosphere containing 5% CO_2 . Non-adherent cells were removed, and adherent cells were passaged in a fresh medium every three days. Neuronal differentiation was induced by the treatment with 10 μM retinoic acid for 10 days (Dwane et al. 2013).

Determination of cell viability by MTT assay

Cell viability was determined using a thiazolyl blue tetrazolium bromide [3-(4,5-dimethyl-2-thiazolyl)-2,5-diphenyl-2*H*-tetrazolium bromide] (MTT) assay (Mosmann 1983). Differentiated SH-SY5Y cells were seeded into 96-well plates at 5000 cells per well and cultured in DMEM supplemented with 10% FBS at 37 °C, 5% CO_2 . After the treatment with a 10 μM concentration of each novel compound, the plate was incubated for 48 h. After the incubation, 10 μL of the MTT reagent (5 mg/mL) was added to each well. The formazan crystals formed were dissolved by

the addition of 100 μL of DMSO. Absorbance values were measured at 690 and 570 nm using a Biotek Power Wave XS microplate reader. Cell viability was determined as below:

$$\text{Viability} = \frac{\text{Average OD of treated wells} - \text{Average OD of blank wells}}{\text{Average OD of control wells} - \text{Average OD of blank wells}} \times 100$$

Cytotoxicity of compounds

Differentiated SH-SY5Y cells (5000 cells/well) were treated with 10 μM compounds for 48 h, and cytotoxic effects of the compounds were evaluated by the MTT reduction assay.

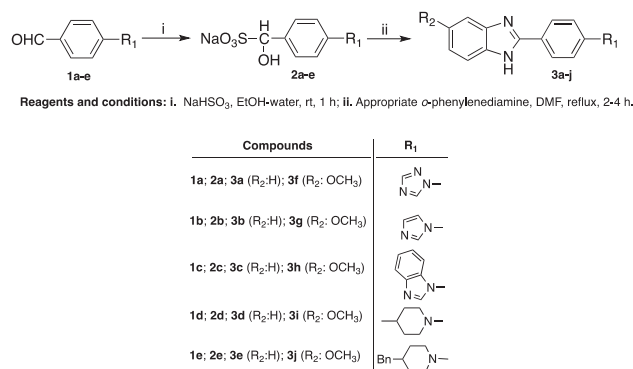
H₂O₂-induced and A β ₁₋₄₀-induced cytotoxicity

For the evaluation of neuroprotective effects of the compounds against the H₂O₂-induced and A β ₁₋₄₀-induced cell death, mitochondrial reduction (MTT) experiments were performed. Differentiated SH-SY5Y cells (5000 cells/well) were treated with 10 μM compounds for 3 h prior to 250 μM H₂O₂ or 10 μM A β ₁₋₄₀ treatment and then incubated for an additional 24 h. The MTT reduction assay was performed to evaluate cell viability (Kim et al. 2000; Loo et al. 1993).

Molecular modeling studies

Docking studies were performed with the Molecular Operating Environment (MOE) version 2015.1001 software available from Chemical Computing Group, Inc. (Montreal, Canada, <http://www.chemcomp.com>) using the crystal structures of human AChE and BChE (Protein Data Bank IDs: 4EY7 (Cheung et al. 2012) and 1P0I (Nicolet et al. 2003), respectively).

After all water and non-protein atoms were removed, the errors in the proteins were corrected by the Structure Preparation process in MOE. Active sites of the enzymes were generated using the Site Finder application. Compound **3g** was constructed using the MOE builder tool, and the energy was minimized using the Merck molecular force field (MMFF94x, gradient: 0.05 kcal mol⁻¹ Å⁻¹). Docking studies for compound **3g** with 4EY7 and 1P0I were performed using the default Triangle Matcher placement method. GBVI/WSA dG, a force field-based scoring function, which estimates the free energy of binding of the ligand from a given pose, was used to rank the final poses. Then the poses with the lowest S score were selected for the enzymes.



Scheme 1 Synthesis of the target compounds

Results and discussion

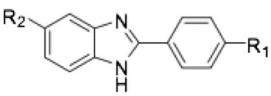
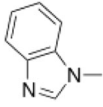
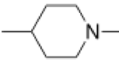
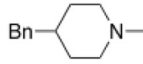
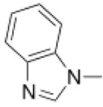
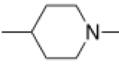
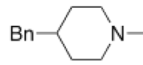
Chemistry

In this study, ten 2-(4-substituted phenyl)-1*H*-benzimidazole derivatives were studied, of which three (**3a–c**) had been described in the literature (Jadhav et al. 2009; Yu et al. 2013; Alp et al. 2014). Compounds **3a–j** were obtained by following the synthetic route outlined in Scheme 1. First, benzaldehydes with aliphatic/aromatic amine moieties (**1a–e**) were synthesized with 45–57 % yield in accordance with a method described in the literature (Meciarova et al. 2003). The intermediates, sodium hydroxy(4-substituted phenyl)methanesulfonate salts (**2a–e**), were obtained with 85–95 % yield by reacting the mentioned benzaldehydes with sodium bisulfite. The target compounds (**3a–j**) were gained with 65–86 % yield by treating sodium hydroxy(4-substituted phenyl)methanesulfonate salts (**2a–e**) with appropriate *o*-phenylenediamines (Alpan et al. 2007). The spectral methods (IR, ¹H/¹³C-NMR, ESI-MS), and elemental analysis were used to elucidate the structures of the compounds that had not been described in the literature (**3d–j**).

In the IR spectra of (**3d–j**), the bands were seen around 1490–1510 cm⁻¹ due to –C=N– stretching. It was very difficult to distinguish the C–H stretching vibrations (around 3300–3100 cm⁻¹) from the broad –NH stretching frequencies (around 3300–2800 cm⁻¹).

In the ¹H NMR spectra, for compounds **3d** and **3e**, the protons on the benzimidazole ring appeared as two multiple peaks at around 7.15 (4-H and 7-H) and 7.55 (5-H and 6-H) p.p.m. For compounds **3f–j**, the signals belonging to 6-H, 4-H, 7-H and methoxy protons on the benzimidazole ring were observed at around 6.90 (dd, *J* = 8.8, 2.4 Hz), 7.15 (d, *J* = 2.4 Hz), 7.55 (d, *J* = 8.8 Hz) and 3.82 p.p.m., respectively. In the ¹³C-NMR spectra, the peaks between 148–151 p.p.m. were assigned to the carbon atoms at the 2 position of benzimidazole ring of the target compounds. The signals appeared at around 55 and 156 p.p.m. in the

Table 1 The physicochemical parameters and in vitro AChE/BChE enzyme inhibition data for the compounds

Compounds			PSA ^a	LogP ^a	MW	H-Bond Don/Accep.	IC ₅₀ (μM) ^b ± SE		Selectivity for BChE ^c
	R ₁	R ₂					BChE	AChE	
3a		H	59.39	1.80	261.28	2/4	>100	>100	
3b		H	46.50	3.06	260.30	2/3	41.35 ± 1.14	67.23 ± 1.11	1.6
3c		H	46.50	4.71	310.36	2/3	74.21 ± 1.20	302 ± 1.67	4
3d		H	31.92	4.52	291.40	2/2	39.56 ± 1.18	>5000	>126
3e		H	31.92	5.89	367.50	2/2	>100	>100	
3f		OCH ₃	68.62	1.79	291.31	2/5	95.44 ± 1.23	471.40 ± 1.24	4.9
3g		OCH ₃	55.73	3.06	290.32	2/4	13.60 ± 1.11	485.70 ± 1.03	35.7
3h		OCH ₃	55.73	4.70	340.39	2/4	14.45 ± 1.31	1051 ± 1.10	72.7
3i		OCH ₃	41.15	4.52	321.42	2/3	15.15 ± 1.25	736.10 ± 1.19	48.5
3j		OCH ₃	41.15	5.89	397.52	2/3	51.20 ± 1.15	>1000	>19
Donepezil							4.94 ± 1.04	6.16 ± 1.03 ^d	

^a PSA and LogP calculated using MOE 2015.1001 (Molecular Operating Environment, Chemical Computing Group)

^b IC₅₀ values of compounds represent the concentration that caused 50% enzyme activity loss

^c Selectivity for BChE is defined as IC₅₀(AChE)/IC₅₀(BChE)

^d IC₅₀ (nM) ± SE

spectra of compound **3f–j**, showed the presence of the methoxy group at the 5 position of benzimidazole ring. Furthermore, the structures of all the target compounds were confirmed by the peaks belonging to [M + Na]⁺ and [M + H]⁺ seen in the ESI mass spectra.

Cholinesterase inhibitory activity

Inhibitory activities of **3a–j** against human recombinant AChE and equine BChE were measured according to the Ellman method. For comparison purposes, donepezil was

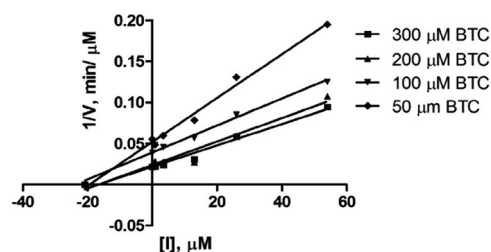


Fig. 2 Dixon plot for non competitive inhibition of BChE by compound **3g**, BTC, r^2 values for the trendlines > 0.95

used as a reference compound. The IC_{50} values of **3a–j** and selectivity indices (SIs) of some compounds for BChE over AChE are summarized in Table 1.

Although, most of the target compounds showed remarkable selective activities for BChE over AChE, none of them exhibited a higher affinity for both AChE and BChE than that of donepezil ($IC_{50} = 6.16$ nM for human AChE and 4.94 μ M for equine BChE), except that **3b** showed balanced inhibition of both ChEs.

Among the target compounds, **3d** and **3g–j** were found as the most potent ($IC_{50} = 13.60–39.56$ μ M) and selective inhibitors of BChE ($SI \geq 35.7$) in this series. Surprisingly, the triazole moiety as a bioisostere of the imidazole moiety decreased the BChE inhibitory activity, as observed for **3a** ($IC_{50} > 100$ μ M) vs. **3b** ($IC_{50} = 41.35$ μ M) and **3f** ($IC_{50} = 95.44$ μ M) vs. **3g** ($IC_{50} = 13.60$ μ M). On the other hand, compounds with the 4-methyl piperidine moiety (**3d** and **3i**) showed interesting potency and selectivity profiles. This significant potency was lost by the replacement of the methyl group with the benzyl group, as observed for **3d** ($IC_{50} = 39.56$ μ M) vs. **3e** ($IC_{50} > 100$ μ M) and **3i** ($IC_{50} = 15.15$ μ M) vs. **3j** ($IC_{50} = 51.20$ μ M). Moreover, introduction of a methoxy group to the benzimidazole ring significantly increased inhibitory activity and selectivity of the compounds against BChE, except **3d** and its counterpart **3i**.

In the BChE inhibition studies, 5-methoxy-2-(4-(1*H*-imidazol-1-yl)phenyl)-1*H*-benzo[*d*]imidazole **3g** was found to be the most active ($IC_{50} = 13.60$ μ M). For this reason, **3g** was selected for further kinetic analysis. The Dixon plot of **3g** for BChE indicated the inhibition type as non competitive (Fig. 2) with K_i values 20.79 ± 3.22 μ M ($r^2 = 0.9751$).

Inhibition of self-mediated $A\beta_{1-40}$ aggregation

The compounds with BChE inhibitory activity ($IC_{50} < 100$ μ M) were further examined for their $A\beta$ -antiaggregating activity and neuroprotective properties. The compounds were tested for their ability to inhibit self-mediated $A\beta_{1-40}$ aggregation using the ThT fluorescence assay. Rifampicin and donepezil were used as reference compounds. The results are summarized in Table 2. Based on the results, none of the compounds was found as effective as the

Table 2 Inhibition of self-mediated $A\beta_{1-40}$ aggregation and cytotoxicity of the compounds

Compounds	$A\beta_{1-40}$ aggregation inhibition (%) \pm SEM	Cell viability (%)
3a	nd	nd
3b	> 100	146
3c	> 100	154
3d	67.78 ± 0.16	135
3e	nd	nd
3f	> 100	172
3g	> 100	229
3h	92.35 ± 0.90	185
3i	75.82 ± 0.99	211
3j	68.39 ± 0.15	169
Control ^a	100	100
Rifampicin	48.40 ± 0.30	106
Donepezil	83.38 ± 0.04	105

^a Control of each assay was individual as non treated.

nd not determined.

standard compound, rifampicin (48.40%). Furthermore, it was determined that **3d**, **3i**, and **3j** (67.78, 75.82, and 68.39%, respectively) showed more potent activity on $A\beta$ aggregation than donepezil (83.38%).

Cytotoxicity

No evidence of cytotoxicity to SH-SY5Y cells exposed to a 10 μ M concentration of the test compounds was observed using the 3-(4,5-dimethylthiazol-2-yl)-2,5-diphenyltetrazolium bromide (MTT) assay. The percentage of growth of the cells is reported in Table 2.

Neuroprotection

The MTT assay was performed to evaluate the neuroprotective effects of the compounds against H_2O_2 -induced and $A\beta_{1-40}$ -induced cell death in SH-SY5Y cells by using rifampicin and donepezil as reference compounds.

When the results of H_2O_2 -induced cytotoxicity were examined, it was seen that protective effects of the tested compounds were significantly higher than that of donepezil. Among them, **3b** and **3d** displayed more protective effect against H_2O_2 -induced cytotoxicity at a concentration of 250 μ M than rifampicin and donepezil (Fig. 3a).

$A\beta_{1-40}$ -induced cytotoxicity results showed that **3c** and **3d** have the highest protective effect against $A\beta_{1-40}$ -induced cytotoxicity at a concentration of 10 μ M (Fig. 3b). Furthermore, the protective effects of the tested compounds were higher than those of rifampicin (except **3i** and **3j**) and donepezil.

Fig. 3 Neuroprotective effect of compounds on H₂O₂-induced and A β ₁₋₄₀-induced cytotoxicity in SH-SY5Y cells. **a** Cells were treated with 250 μ M H₂O₂ in the presence or absence of compounds (10 μ M) at 24 hours. **b** Cells were treated with 10 μ M A β ₁₋₄₀ in the presence or absence of compounds (10 μ M) at 24 hours. The values are the mean values \pm SEM from at least three independent experiments. * $p < 0.05$

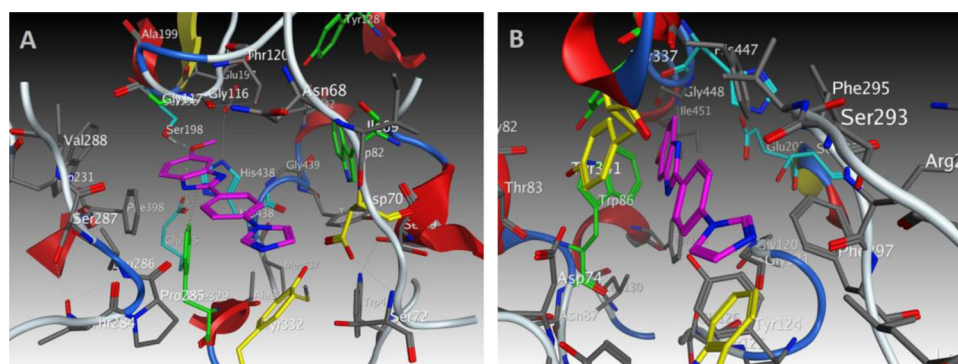
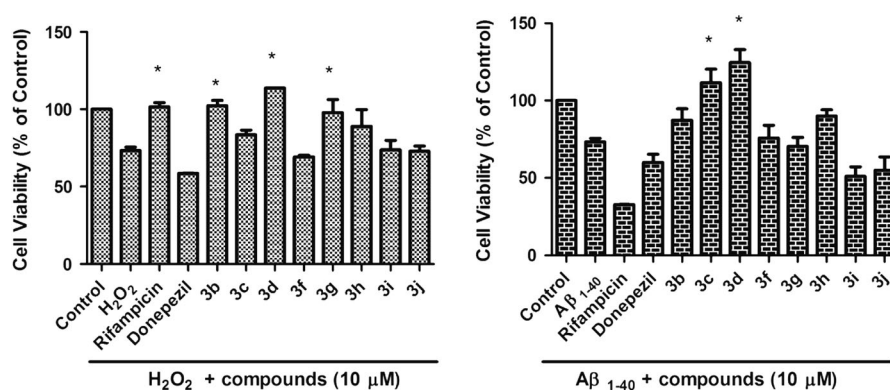


Fig. 4 **a** Representation of the binding mode of **3g** (purple) in the BChE active site. The catalytic triad (Ser198, His438, and Glu325) is shown in blue, the anionic site (Trp82, Tyr128, and Phe329) is shown in green, and the peripheral anionic site (Tyr332 and Asp70) is shown in yellow. **b** Representation of the binding mode of **3g** (purple) in the

AChE active site. The catalytic triad (Ser203, His447, and Glu402) is shown in blue, the anionic site (Trp86 and Tyr337) is shown in green, and the peripheral anionic site (Trp286 and Tyr341) is shown in yellow (color figure online)

Molecular modeling

To predict the drug-likeness of the designed compounds, the Lipinski's rule of five was calculated. All the compounds conformed to the rule of five, except **3e** and **3j** (Table 1). The passage through the blood–brain barrier (BBB) is a major issue for central nervous system-acting drugs. It has been hypothesized that the polar surface area (PSA) of a compound that passes the BBB should be typically less than 70 \AA^2 (Muchmore et al. 2010; Pajouhesh and Lenz 2005). The calculated PSA values of the designed compounds were found to be between 31 to 68 \AA^2 (Table 1). This finding may suggest that, according to this hypothesis, the compounds are able to pass the BBB.

Compared to AChE, BChE, in which two phenylalanine residues are replaced with smaller amino acids, valine and leucine, allows larger molecules to get in. The docking studies revealed that the most active compound, **3g**, is accommodated in the catalytic site of the BChE active pocket (Fig. 4a). A hydrogen bond is formed between the methoxy moiety of **3g** and the hydroxyl group of Ser198

(one of the catalytic triad residues). Besides, a CH— π interaction, which can be classified as a weak hydrogen bond (Brandl et al. 2001), occurred between Phe329 and the benzimidazole ring in the anionic site. The determined orientation and interactions might be responsible for the inhibitory activity of **3g**.

From the docking studies with AChE, it was seen that **3g** did not pass the gorge to reach the catalytic or anionic site. In addition, there was no appropriate interaction between AChE and **3g** (Fig. 4b). It can be inferred that these compounds cannot inhibit AChE because AChE has a narrow gorge, and the compounds do not have the conformational flexibility to pass this narrow gorge.

Conclusion

In conclusion, a series of 2-phenylbenzimidazoles have been designed, synthesized, and evaluated for their ChE inhibitory activities in this study. The target compounds (**3a–j**) were obtained by cyclization of *o*-phenylenediamines with

sodium hydroxy(4-substituted phenyl)methanesulfonate salts. In vitro studies indicated that the most of the target compounds showed remarkable inhibitory activity against BChE (IC_{50} : 13.60–95.44 μ M). Among them, **3d** and **3g-i** also exhibited high selectivity ($SI \geq 35.7$) for BChE with IC_{50} values 39.56, 13.60, 14.45, and 15.15 μ M, respectively. Furthermore, kinetic studies of the compound **3g** showed non competitive type of inhibition. Molecular docking studies were also performed to gain a better understanding of possible interactions between the most active compound and the ChEs. It may be assumed that the compounds can reach the catalytic anionic site of the BChE active site. It is worth mentioning that the compounds cannot pass the narrow gorge of the AChE active site due to their rigid structures. The compounds with BChE inhibitory activity were subsequently evaluated for their $A\beta_{1-40}$ -anti-aggregating activity and neuroprotective properties using SH-SY5Y cells. Among the compounds, **3d** not only inhibited the $A\beta_{1-40}$ aggregation but also demonstrated significant neuroprotection against H_2O_2 -induced and $A\beta_{1-40}$ -induced cell death. Collectively, compound **3d** showed the best multifunctional activity (BChE; $IC_{50} = 39.56 \mu$ M, $SI > 126$; $A\beta$ self-mediated aggregation; 67.78% at 100 μ M; H_2O_2 -induced cytotoxicity with cell viability of 98% and $A\beta_{1-40}$ -induced cytotoxicity with cell viability of 127%). All these results suggested that 2-(4-(4-methylpiperidin-1-yl)phenyl)-1H-benzo[d]imidazole (compound **3d**) could be a promising multi-target lead candidate against AD.

Acknowledgements The authors gratefully acknowledge the financial support of the Turkish Scientific Research Institution (TUBITAK, 114S374).

Conflict of interest The authors declare that they have no conflict of interests.

References

- Alp M, Goker AH, Altanlar N (2014) Synthesis and antimicrobial activity of novel 2-[4-(1H-benzimidazol-1-yl)phenyl]-1H-benzimidazoles. *Turk J Chem* 38:152–156
- Alpan AS, Gunes HS, Topcu Z (2007) 1H-Benzimidazole derivatives as mammalian DNA topoisomerase I inhibitors. *Acta Biochim Pol* 54:561–565
- Alpan AS, Parlar S, Carlino L, Tarikogullari AH, Alptuzun V, Gunes HS (2013) Synthesis, biological activity and molecular modeling studies on 1H-benzimidazole derivatives as acetylcholinesterase inhibitors. *Bioorg Med Chem* 21:4928–4937
- Anand P, Singh B (2013) A review on cholinesterase inhibitors for Alzheimer's disease. *Arch Pharm Res* 36:375–399
- Bansal Y, Silakari O (2012) The therapeutic journey of benzimidazoles: a review. *Bioorg Med Chem* 20(21):6208–6236
- Brandl M, Weiss MS, Jabs A, Suhnel J, Hilgenfeld R (2001) C-H center dot center dot center dot pi-interactions in proteins. *J Mol Biol* 307:357–377
- Bullock R, Touchon J, Bergman H, Gambina G, He Y, Rapatz G, Nagel J, Lane R (2005) Rivastigmine and donepezil treatment in moderate to moderately-severe Alzheimer's disease over a 2-year period. *Curr Med Res Opin* 21:1317–1327
- Cheung J, Rudolph MJ, Burshteyn F, Cassidy MS, Gary EN, Love J, Franklin MC, Height JJ (2012) Structures of human acetylcholinesterase in complex with pharmacologically important ligands. *J Med Chem* 55:10282–10286
- Cui M, Ono M, Kimura H, Kawashima H, Liu BL, Saji H (2011) Radioiodinated benzimidazole derivatives as single photon emission computed tomography probes for imaging of beta-amyloid plaques in Alzheimer's disease. *Nucl Med Biol* 38:313–320
- Cummings JL (2004) Drug therapy – Alzheimer's disease. *New Engl J Med* 351:56–67
- Darvesh S, Reid GA (2016) Reduced fibrillar beta-amyloid in subcortical structures in a butyrylcholinesterase-knockout Alzheimer disease mouse model. *Chem Biol Interact* 259(B):307–312
- Dwane S, Durack E, Kiely PA (2013) Optimising parameters for the differentiation of SH-SY5Y cells to study cell adhesion and cell migration. *BMC Res Notes* 6:366–376
- Ellman GL, Courtney KD, Andres V, Featherstone RM (1961) A new and rapid colorimetric determination of acetylcholinesterase activity. *Biochem Pharmacol* 7:88–95
- Giacobini E (2003) Cholinesterases: new roles in brain function and in Alzheimer's disease. *Neurochem Res* 28:515–522
- Gouras GK, Olsson TT, Hansson O (2015) Beta amyloid peptides and amyloid plaques in Alzheimer's disease. *Neurotherapeutics* 12(1):3–11
- Harada R, Okamura N, Furumoto S, Yoshikawa T, Arai H, Yanai K, Kudo Y (2014) Use of a benzimidazole derivative BF-188 in fluorescence multispectral imaging for selective visualization of tau protein fibrils in the Alzheimer's disease brain. *Mol Imaging Biol* 16:19–27
- Holmes C, Ballard C, Lehmann D, Smith AD, Beaumont H, Day IN, Khan MN, Lovestone S, McCulley M, Morris CM, Munoz DG, O'Brien K, Russ C, Del Ser T, Warden D (2005) Rate of progression of cognitive decline in Alzheimer's disease: effect of butyrylcholinesterase K gene variation. *J Neurol Neurosurg Psychiatry* 76:640–643
- Huang WJ, Zhang X, Chen WW (2015) Role of oxidative stress in Alzheimer's disease. *Biomed Rep* 4(5):519–522
- Jadhav GR, Shaikh MU, Kale RP, Gill CH (2009) Ammonium metavanadate: a novel catalyst for synthesis of 2-substituted benzimidazole derivatives. *Chinese Chem Lett* 20:292–295
- Karran E, Mercken M, Strooper B (2011) The amyloid cascade hypothesis for Alzheimer's disease: an appraisal for the development of therapeutics. *Nat Rev Drug Discov* 10:698–712
- Kim KD, Cho ES, Um HD (2000) Caspase-dependent and -independent events in apoptosis induced by hydrogen peroxide. *Exp Cell Res* 257(1):82–88
- Loo DT, Copani A, Pike CJ, Whittemore ER, Walencewicz AJ, Cotman CW (1993) Apoptosis is induced by beta-amyloid in cultured central nervous system neurons. *Proc Natl Acad Sci USA* 90(17):7951–7955
- Manev H, Chen H, Dzitoyeva S, Manev R (2011) Cyclooxygenases and 5-lipoxygenase in Alzheimer's disease. *Prog Neuropsychopharmacol Biol Psychiatry* 35:315–319
- Meciarova M, Toma S, Magdolen P (2003) Ultrasound effect on the aromatic nucleophilic substitution reactions on some haloarenes. *Ultrason Sonochem* 10:265–270
- Mosmann T (1983) Rapid colorimetric assay for cellular growth and survival: application to proliferation and cytotoxicity assays. *J Immunol Methods* 65(1-2):55–63
- Muchmore SW, Edmunds JJ, Stewart KD, Hajduk PJ (2010) Cheminformatic tools for medicinal chemists. *J Med Chem* 53:4830–4841

- Mullard A (2017) Alzheimer amyloid hypothesis lives on. *Nat Rev Drug Discov* 16:3–5
- Nicolet Y, Lockridge O, Masson P, Fontecilla-Camps JC, Nachon F (2003) Crystal structure of human butyrylcholinesterase and of its complexes with substrate and products. *J Biol Chem* 278:41141–41147
- Oddo S, Caccamo A, Kitazawa M, Tseng BP, LaFerla FM (2003) Amyloid deposition precedes tangle formation in a triple transgenic model of Alzheimer's disease. *Neurobiol Aging* 24:1063–1070
- Pajouhesh H, Lenz GR (2005) Medicinal chemical properties of successful central nervous system drugs. *NeuroRx* 2:541–553
- Perry E, Perry R, Blessed G, Tomlinson B (1978) Changes in brain cholinesterases in senile dementia of Alzheimer type. *Neuropathol. Appl. Neurobiol* 4:273–277
- Reid GA, Darvesh S (2015) Butyrylcholinesterase-knockout reduces brain deposition of fibrillar β -amyloid in an Alzheimer mouse model. *Neuroscience* 298:424–435
- Secci D, Bolasco A, D'Ascenzio M, Sala F, Yáñez M, Carradori S (2012) Conventional and microwave-assisted synthesis of benzimidazole derivatives and their in vitro inhibition of human cyclooxygenase. *J Heterocyclic Chem* 49:1187–1195
- Selkoe DJ, Hardy J (2016) The amyloid hypothesis of Alzheimer's disease at 25 years. *EMBO Mol Med* 8:595–608
- Sun X, Chen WD, Wang YD (2015) β -Amyloid: the key peptide in the pathogenesis of Alzheimer's disease. *Front Pharmacol* 6:221–229
- Taylor JP, Hardy J, Fischbeck KH (2002) Toxic proteins in neurodegenerative disease. *Science* 296:1991–1995
- Yadav G, Ganguly S (2015) Structure activity relationship (SAR) study of benzimidazole scaffold for different biological activities: a mini-review. *Eur J Med Chem* 97:419–443
- Yiannopoulou KG, Papageorgiou SG (2013) Current and future treatments for Alzheimer's disease. *Ther Adv Neurol Disord* 6(1):19–33
- Yoon YK, Ali MA, Wei AC, Choon TS, Khaw KY, Murugaiyah V, Osman H, Masand VH (2013) Synthesis, characterization, and molecular docking analysis of novel benzimidazole derivatives as cholinesterase inhibitors. *Bioorg Chem* 49:33–39
- Yu Z, Zheng Z, Yang M, Wang L, Tian Y, Wu J, Zhou H, Xu H, Wu Z (2013) Photon-induced intramolecular charge transfer with the influence of D/A group and mode: optical physical properties and bio-imaging. *J Mater Chem C* 1:7026–7033
- Zhu JM, Wu CF, Li XB, Wu GS, Xie S, Hu QN, Deng ZX, Zhu MX, Luo HR, Hong XC (2013) Synthesis, biological evaluation and molecular modeling of substituted 2-aminobenzimidazoles as novel inhibitors of acetylcholinesterase and butyrylcholinesterase. *Bioorg Med Chem* 21:4218–4224